NASA TECHNICAL MEMORANDUM 100577
AVSCOM TECHNICAL MEMORANDUM 88-B-011

CHARACTERIZATION OF MODE I AND MODE II DELAMINATION GROWTH AND THRESHOLDS IN GRAPHITE/PEEK COMPOSITES

RODERICK H. MARTIN
AND
GRETCHEN B. MURRI

APRIL 1988

NASA
National Aeronautics and Space Administration
Langley Research Center
Hampton, Virginia 23665

US ARMY AVIATION SYSTEMS COMMAND
AVIATION R&T ACTIVITY

SUMMARY

Composite materials often fail by delamination. As composite materials with tougher matrices are developed to give better delamination resistance, their delamination behavior needs to be fully characterized. In this paper the onset and growth of delamination in AS4/PEEK, a tough thermoplastic matrix composite, was characterized for mode I and mode II loadings, using the Double Cantilever Beam (DCB) and the End-notched Flexure (ENF) test specimens, respectively. Delamination growth per fatigue cycle, da/dN, was related to strain energy release rate, G , by means of a power law. However, the exponents of these power laws were too large for them to be adequately used as a life prediction tool. A small error in the estimated applied loads could lead to large errors, at least one order of magnitude, in the delamination growth rates. Hence strain energy release rate thresholds, G_{th} , below which no delamination would occur were also measured. Mode I and II threshold G values for no delamination growth were found by monitoring the number of cycles to delamination onset in the DCB and ENF specimens. The maximum applied G for which no delamination growth had occurred until at least 10^6 cycles was considered the threshold strain energy release rate. The G_{th} values for both mode I and mode II were much less than their corresponding fracture toughnesses. Results show that for specimens that had been statically pre-cracked in shear have similar G_{th} values for mode I and mode II for R ratios of 0.1 and 0.5. An expression was developed which relates G_{th} and G_c to cyclic delamination growth rate. Comments are given on how testing effects, e.g. facial

interference and damage ahead of the delamination front, may invalidate the experimental determination of the constants in the expression.

KEYWORDS

composite materials, fracture mechanics, Double Cantilever Beam, End-notched Flexure, delamination, fatigue, threshold, strain energy release rate

NOMENCLATURE

A	Constant in delamination characterization power laws
a	Delamination length
B	Exponent in delamination characterization power laws
b	Beam width
C	Beam compliance
D_1, D_2	Exponents in delamination characterization power law
E	Axial modulus of laminate in fiber direction
G	Total strain energy release rate
G_c	Fracture toughness
G_I	Mode I strain energy release rate
G_{II}	Mode II strain energy release rate
G_{Ic}	Interlaminar fracture toughness in tension
G_{IIc}	Interlaminar fracture toughness in shear
G_{Imax}	Maximum cyclic strain energy release rate for delamination due to interlaminar tension
G_{IImax}	Maximum cyclic strain energy release rate for delamination due to interlaminar shear
G_{min}	Minimum cyclic strain energy release rate
G_{max}	Maximum cyclic strain energy release rate
G_{th}	Total maximum cyclic strain energy release rate for no delamination growth in fatigue
G_{Ith}	Maximum cyclic G_I for no delamination growth in fatigue
G_{IIth}	Maximum cyclic G_{II} for no delamination growth in fatigue
ΔG	Total strain energy release rate range, $(G_{max}-G_{min})$

h	Beam half-thickness
I	Beam moment of inertia
L	Half-span of ENF specimen
m	Compliance calibration constant for mode I specimen
N	Number of fatigue cycles
n	Compliance calibration exponent for mode I specimen
P	Applied load
P_{max}	Maximum cyclic applied load for delamination in fatigue
R	Ratio of minimum to maximum cyclic displacements
r	Compliance calibration constant for mode II specimen
s	Compliance calibration constant for mode II specimen
δ	Load point displacement
δ_{max}	Maximum cyclic load point displacement

INTRODUCTION

As the use of fiber reinforced materials in primary aircraft structures increases, the damage tolerance of such materials becomes increasingly important. The most common failure mechanism in laminated composites is delamination [1-5]. Thus, the ability to predict delamination behavior is important for establishing static and dynamic damage tolerance criteria. Furthermore, the accuracy of the damage characterization techniques used will determine the accuracy of the failure predictions.

One way of improving the resistance to delamination of laminated composite materials is to use tough matrices such as thermoplastics [1]. One such thermoplastic material is PEEK, Poly(etheretherketone). Since the introduction of PEEK in laminated composite form (APC-1 and APC-2) by Imperial Chemical Industries (ICI), it has typically been found to have inconsistent properties. Hence previous attempts to characterize delamination of APC-2 [3,4,6] have been subject to material variations from investigator to investigator . However, a data base on the mechanical properties of APC-2 has now been provided [7] because the manufacturing processes have been sufficiently standardized. There is, therefore, a need to re-characterize the delamination behavior of the most recent form of APC-2.

Recently, APC-2 has been included in a round robin test program conducted by an ASTM task group investigating fracture toughness tests for the purpose of developing standards for static mode I and mode II fracture

toughness measurements. (Supporting data available from ASTM Headquarters. Request RR D30.02.02.) It is equally important to develop testing standards for characterizing delamination growth under cyclic loading. However, to date there is no recommended procedure for cyclic delamination characterization. Therefore, in this study, Double Cantilever Beam (DCB) and End-notched Flexure (ENF) specimens were used to characterize cyclic mode I (opening or peel) and mode II (sliding or interlaminar shear) delamination, respectively. This study and other work in the literature on delamination characterization of composite materials may be useful for developing cyclic delamination test standards.

Fatigue crack growth in metals can be characterized by relating crack growth per cycle to the cyclic stress intensity factor range, ΔK , [8]. For composite materials, delamination growth has been related to the cyclic strain energy release rate [2-6] using a power law. For composites, the exponents for relating propagation rate to strain energy release rate have been shown to be high [3,4], especially in mode I. With large exponents, small uncertainties in the applied loads will lead to large uncertainties (at least one order of magnitude) in the predicted delamination growth rate. This makes the derived power law relationships unsuitable for design purposes. Hence, for composite materials more emphasis must be placed on the strain energy release rate threshold. Therefore, it is important to ensure that the threshold value obtained corresponds to no delamination growth in the structure.

Reference 9 presents extensive studies on obtaining crack growth thresholds in metals. Typically the threshold in metals is found by reducing the applied loads until the crack growth arrests. However, for composite materials a threshold value determined by delamination arrest may

be unconservative because it may depend on the load history of the specimen. There is a more convenient and potentially more accurate method for determining a conservative G_{th} in composite materials. Reference 10 found a no-growth threshold value of strain energy release rate for debonding in adhesively bonded joints by monitoring the number of cycles to debond growth onset. In references 11 through 13 delamination growth onset in Edge Delamination Tests (EDT) and End notched Flexure (ENF) tests were used to generate no-delamination-growth G thresholds. In these studies, it was assumed that if the delamination had not begun to grow after 1 million cycles, the applied load and hence the corresponding G , could be considered below a threshold value.

Therefore to fully characterize the cyclic delamination growth of APC-2 in this study, two things were done. First, a power law relationship between delamination growth and strain energy release rate for the most current version of APC-2 was determined. Then the threshold values of strain energy release rate were determined by monitoring the number of cycles to delamination growth onset. For a no-delamination-growth design, as proposed by O'Brien [11], the structure is assumed to have no load history, and structural discontinuities such as edges, ply drops, matrix cracks, inserts etc., are assumed to act as delamination initiators. For this study inserts and pre-cracks were used to simulate existing delaminations.

In the DCB tests under displacement control, the delamination growth rate started at a high value and decreased as the delamination grew. At a displacement ratio (R ratio) of R=0.1 the tests were continued until the delamination growth rate was less than 10^{-8} in/cycle and the delamination growth was assumed to have arrested. The value of maximum cyclic strain

energy release rate at delamination growth arrest is compared with the threshold value of strain energy release rate obtained from monitoring the number of cycles to delamination growth onset. Finally, a delamination growth rate expression is postulated for the entire range of G_{max}, from the threshold strain energy release rate to the fracture toughness for either mode I or mode II.

MATERIALS

The specimens were cut from the same panels as the specimens used in the ASTM Round Robin, and the Round Robin testing guidelines were followed wherever applicable. Both mode I and mode II specimens were unidirectional, 36-ply APC-2 (AS4/PEEK) laminates. All specimens were approximately one inch wide and had a nominal thickness, 2h, of 0.180 inches. To simulate an initial delamination in each specimen, a piece of folded aluminum foil was inserted at the mid-plane at one end of each specimen during the layup of the pre-preg. The total insert thickness was 0.005 inches.

The average fiber volume fraction of the specimens was 64 percent. The crystallinity of the PEEK in the panels used in this study was measured by wide angle X-ray diffraction techniques [14]. The crystalline percentage varied from 21.5 to 23.8 percent. Before testing, the specimens were vacuum dried for approximately 20 hours, according to the drying cycle recommended for the ASTM Round Robin. This consisted of heating for 1 hour at 200°F, 1 hour at 225°F, 16 hours at 250°F, and 1 hour at 300°F. The specimens were allowed to cool to room temperature and then tested or stored in a dessicator for several days prior to testing.

For these specimens, the range of the mode I static fracture toughness, G_{Ic}, from the preliminary results of the ASTM Round Robin test program is $9.65 \leq G_{Ic} \leq 14.14$ in-lb/in^2. The range of the mode II static fracture toughness, also from the preliminary results of the ASTM Round Robin, is $14.2 \leq G_{IIc} \leq 21.5$ in-lb/in^2.

TEST TECHNIQUES AND PROCEDURES

Both the DCB and ENF tests were conducted under displacement control in a servo-hydraulic test stand. All fatigue tests were conducted at a frequency of 5 Hertz. Two different displacement ratios (R ratios) were used: R=0.1 and R=0.5. To make the delamination more visible during testing, the sides of the specimens were coated with a water-based, brittle typewriter correction fluid and marks were made at 0.1 inch intervals from the initial delamination tip. An optical microscope and light source were used to enhance observation of the delamination growth.

For the delamination onset tests the folded aluminum insert in the specimens used in this study provided a straight delamination front with no load history. However, the 0.005 inch insert provided a blunt delamination tip with a resin pocket extending into the undelaminated part of the specimen [15] and thus does not truly represent delamination of a laminated composite material. Therefore, delamination onset tests were conducted on DCB specimens with a static shear pre-crack and were compared to tests run on specimens where the delamination grew from the insert. A static shear pre-crack was used to prevent fiber bridging. Previous studies using the ENF test to measure the mode II critical strain energy release rate, G_{IIc},

have shown that testing from the insert can give significantly higher values of G_{IIc} than tests for which the specimen was pre-cracked to extend the initial delamination beyond the tip of the insert [15]. Hence for static ENF tests some form of pre-crack is normally used in order to determine the most conservative values of G_{IIc}. Therefore, all ENF test specimens were statically pre-cracked in shear prior to all fatigue tests. The effect of the pre-cracking is discussed later.

Double Cantilever Beam Tests

Figure 1 shows the DCB specimen, with hinge tabs through which the load is applied. The hinge tabs were bonded to the specimen with Hysol EA9309, a two part, room temperature cure adhesive. The vacuum drying cycle was applied to the specimen after the hinge adhesive had cured and may also have acted as a post cure. The beam opening displacement, δ, was measured using the stroke of the machine which was monitored using a digital voltmeter. The machine compliance was assumed to be negligible.

The DCB test is the most commonly used method for characterizing mode I fracture toughness. However, this test has many limitations which influence its ability to accurately measure static fracture toughness, G_{Ic}. These problems include fiber bridging [5,16,17], geometric nonlinearity [18,19], loading rate effects [20-22] and material plasticity [23,24]. There is little published work dealing with how these inherent problems may affect the fatigue response of the DCB specimen.

Fiber bridging has been shown to increase resistance to delamination in static DCB testing. In fatigue testing the delamination growth may also be

inhibited by fiber bridging and the measured strain energy release rate threshold may increase with increasing amounts of fiber bridging. Some fiber bridging was noticeable in the ASTM Round Robin testing of APC-2; however, the amount was small in comparison to graphite/epoxy laminates. An example of the fiber bridging problems in graphite/epoxy laminates is given in reference 17.

Geometric non-linearity influences the strain energy release rate in DCB specimens when the moment arms of the cantilever are shortened by bending. In fatigue, the ratio of opening displacement, δ , to delamination length, a , is constantly changing, so a correction factor, as suggested for static testing in reference 19, is difficult to apply. However, geometric non-linearity has a greater effect at high δ/a ratios. In fatigue, it is simpler to keep the δ/a ratio low rather than to apply a correction factor. This can be done by using thick beams (24 or more plies) and by testing at small delamination lengths (less than 3 inches). Both of these techniques were used in the current tests.

Preliminary results of the ASTM Round Robin test program showed that the amount of material non-linearity in the APC-2 DCB specimen was small and localized at the delamination front during static tests. Therefore, it was assumed that plasticity could be ignored in the current fatigue testing, where the maximum cyclic loads and displacements are usually far less than the critical values under monotonic loading.

When the DCB becomes unloaded in a fatigue cycle the delaminated faces come in contact, resulting in facial interference. Facial interference is a combination of effects including fiber bridging, a plasticity zone wake (usually called crack closure in metals), rough surfaces and debris. All of these aid in artificially closing the delamination during unloading in the

fatigue cycle. This effect can appear on a static load-displacement plot as part of a permanent residual displacement [24]. Facial interference has the largest effect on G_{min} as the R-ratio approaches zero. Because of this uncertainty in the G_{min} value, G_{max} was used as the independent variable in this study rather than ΔG , or $(G_{max}-G_{min})$.

End-notched Flexure Tests

Figure 2 shows a schematic of the ENF specimen. For this study L=2 inches. The test set-up is shown in fig. 3. Load was applied to the ENF specimen by loading rollers in a three point bend test fixture. The rollers were mounted on ball-bearings and hence were free to rotate. The displacement is measured by a direct-current differential transducer (DCDT) mounted under the center of the specimen with the rod supported by a spring. This method eliminates the need to consider the effect of machine compliance on the data. A "restraining bar" is visible in fig. 3 at the un-delaminated end of the specimen. Because the specimen is delaminated at one end only, it will deflect asymmetrically, resulting in small side forces which tend to shift the specimen on the roller fixtures. The restraining bar prevents shifting of the specimen as it is loaded and is free to rotate as the specimen deforms during the test. The specimens were tested with the initial delamination front approximately mid-way between the outer and center load lines (a=1 inch) to avoid stress concentrations caused by the loading rollers.

A compliance calibration was performed on each ENF specimen prior to testing. After pre-cracking, the specimen was placed in the test fixture at

four different a/L ratios and loaded sufficiently to produce a linear load-displacement plot but not high enough to extend the delamination. The slopes of the load-displacement plots for each delamination length were measured and linear regression was used to fit a relationship between compliance and delamination length for each specimen. This compliance calibration reduced possible errors caused by different responses of individual specimens.

Pre-cracking in Shear

Shear pre-cracks were initiated in the DCB and ENF specimens by positioning the specimens in the ENF loading fixture so that a/L was just less than 1. The specimen was then loaded statically, causing the delamination front to extend to a point under the central loading roller. This technique provided a sharp delamination front.

After pre-cracking, an optical microscope and light source were used to locate the new delamination tip. The accuracy of this technique was verified by breaking open a few tested specimens and examining the surfaces. Since the static and fatigue surfaces look distinctly different, it was easy to locate the actual pre-crack tip and compare it with the location on the edge of the specimen obtained using the microscope. The microscope proved to be excellent for locating the delamination tip. The initial delamination lengths, a, for all the tests were determined using the microscope.

Delamination Growth Rate Determination

As a delamination grows at a constant cyclic displacement, the cyclic G changes, hence the delamination growth rate changes. A plot of da/dN versus G may be obtained by testing a specimen at a cyclic G_{max} less than the static fracture toughness. This method was used to obtain plots of G_{Imax} and G_{IImax} versus da/dN.

For the DCB specimen stable delamination growth occurs under static displacement control because dG/da is always negative [25]. Therefore both the strain energy release rate and the delamination growth rate, da/dN, will decrease as the delamination grows. Thus, tests were conducted at an initial G_{Imax} just less than G_{Ic}. At R=0.1 the tests were continued until delamination arrest occurred. Then the tests were continued an additional one million cycles to verify that the delamination had fully arrested.

For the ENF specimen, even under displacement control, static delamination growth is unstable for the useful portion of the beam because dG/da is positive [25]. In fatigue as the delamination grows with cycles, the strain energy release rate increases, and the delamination growth rate increases. Therefore, all the ENF fatigue tests were started at a low maximum cyclic strain energy release rate. Thus, cycles were necessary to start delamination growth from the static pre-crack. The number of loading cycles to delamination growth onset was monitored in each test.

Delamination growth rates, da/dN , were computed by calculating the slope of the straight line connecting two adjacent points on the a versus N curve. This approximation is reasonable if the delamination length increments are small.

Delamination Growth Onset Determination

In reference 13, the number of cycles to delamination onset of an ENF specimen was determined by visually observing delamination growth at the specimen edges. A similar technique was used for mode I and mode II testing in this study. For the tests in both modes the maximum cyclic load was monitored with a digital voltmeter. A one to two percent decrease in the load at a constant maximum displacement indicated that the delamination had begun to grow. Delamination growth onset was verified using an optical microscope and the number of cycles to delamination growth onset was recorded. For the mode II tests, for each specimen, the number of cycles to delamination growth onset was recorded and the testing was continued to determine the cyclic growth rate data as described above. For the mode I tests, individual specimens were used separately to measure either delamination growth onset or delamination growth rate.

ANALYSIS

The following section introduces the expressions used to calculate the mode I and II strain energy release rate. Brief derivations are given, and references are cited containing the full derivations.

Double-Cantilever Beam Test

The compliance of the DCB can be shown to be equal to a power law function of the delamination length [26] of the form,

$$\frac{\delta}{P} = C = m\,a^{n} \qquad (1)$$

where δ is the displacement of the specimen at the point of load application, P is the applied load, a is the delamination length, and m and n are constants found by plotting experimental values of log C versus log a. Classical beam theory expressions would give values of $n = 3$ and $m = 2/(3EI)$. However, beam theory makes several assumptions that may not be true in experimental testing. Therefore, the experimental and theoretical values of m and n may differ. Hence, in this work the constants m and n found from the ASTM Round Robin experimental data were used to calculate static compliance. The values of m and n used in this work were $m=8.831\times10^{-4}$ and $n=2.723$, where the units of a in equation (1) are inches and the units of compliance are in/lb.

The delamination strain energy release rate can be expressed as [26]

$$G = \frac{P^2}{2b}\,\frac{dC}{da} = \frac{\delta^2}{2bC^2}\,\frac{dC}{da} \qquad (2)$$

where b is the specimen width. Differentiating equation (1) with respect to a yields

$$\frac{dC}{da} = n\,m\,a^{n-1} = \frac{n\,C}{a} \qquad (3)$$

Substituting equation (1) and equation (3) into equation (2) yields the maximum cyclic strain energy release rate as

$$G_{Imax} = \frac{n\, P_{max} \delta_{max}}{2\, b\, a} \qquad (4)$$

End-Notched Flexure Test

An analysis similar to that for the DCB was adopted for the ENF specimen, for which the compliance can be expressed as [27]

$$\frac{\delta}{P} = C = ra^3 + s \qquad (5)$$

The constants r and s can be found by plotting experimental values of C versus a^3. Classical beam theory gives values of $r=1/(4EI)$ and $s=L^3/(6EI)$. The average experimental compliance calibration values used in this work were $r=0.297\times10^{-4}$ and $s=1.505\times10^{-4}$ where the units of a were inches and the units of C were in/lb. The constant r varied from 0.2215×10^{-4} to 0.383×10^{-4} and the constant s varied from 1.226×10^{-4} to 1.623×10^{-4}. The average values from the preliminary results of the ASTM Round Robin were $r = 0.2709\times10^{-4}$ and $s = 1.661\times10^{-4}$.

Differentiating eq.(5) with respect to delamination length, a , and substituting into eq.(2), yields the maximum cyclic strain energy release rate for the ENF specimen as

$$G_{IImax} = \frac{3\, P_{max}^2 r\, a^2}{2b} = \frac{3\, \delta_{max}^2 r\, a^2}{2b\, C^2} \qquad (6)$$

RESULTS AND DISCUSSION

A complete characterization of cyclic delamination of composite materials must include the threshold for no delamination growth, the delamination growth rate and the fracture toughness. Therefore, growth rate results are included here for completeness and as a comparison to other results for APC-2. In this section the cyclic delamination growth rate tests are discussed first. The second part of this section describes the results of the delamination growth onset tests and compares the value of G_{Ith} obtained from these tests with the strain energy release rate at delamination arrest in the DCB at R=0.1. The last article of this section presents a postulated expression for the delamination growth rate which attempts to correlate the above two results with the fracture toughness.

Cyclic Delamination Growth

Mode I Cyclic Growth

The results for mode I cyclic delamination growth at displacement ratios of 0.1 and 0.5 are shown in fig. 4. The straight lines were obtained by a least squares fit of the data points between $da/dN=10^{-7}$ and $da/dN=10^{-4}$ inches per cycle. These limits were chosen to be above the no-growth, or threshold region, and below the the static delamination growth region, respectively. Experimental DCB results for APC-2 for the current study resulted in the following power law relationship:

$$da/dN = A\ G_{Imax}^{B} \qquad (7)$$

where $A = 5.370 \times 10^{-11}$ and $B = 6.14$ at R=0.1, and $A = 3.715 \times 10^{-14}$ and $B = 8.50$ at R=0.5. The delamination growth rate in equation 7 is measured in in/cycle and G_{Imax} is expressed in in-lb/in^2. At R=0.1 the delamination was observed to arrest at a $G_{Imax} = 3$ in-lb/in^2.

Other researchers [3,4,6,28] have used similar methods to characterize the mode I cyclic delamination growth of APC-2 but did not attempt to evaluate a threshold strain energy release rate. Their results are given in Table 1. All the results shown in the table correspond to tests at R=0.1. The scatter of results may be caused by the differences in the manufacturing processes of the APC-2 used and show the importance of developing test standards which will help reduce variations in material properties and test methods used by different laboratories.

Mode II Cyclic Growth

The results for mode II growth at R=0.1 and R=0.5 are shown in fig. 5. The straight lines were obtained by a least squares fit of the data between the limits $10^{-7} < da/dN < 10^{-4}$. As in the DCB, these limits were chosen to be above the threshold region and below the static growth region respectively. Based on these results, the mode II delamination growth rates for APC-2 resulted in the power law relationship

$$da/dN = A\ G_{IImax}^{B} \qquad (8)$$

where $A = 3.311 \times 10^{-7}$, $B = 3.645$ at R=0.1, and $A = 1.660 \times 10^{-9}$, $B = 5.34$ at R=0.5 and da/dN is measured in inches per cycle and G_{IImax} is expressed in in-lb/in^2.

Fig. 5 shows no obvious change of slope at low G_{IImax} for either R ratio. At higher values of G_{IImax} the experimental data points appear to be turning, i.e. the gradient is increasing towards an infinite delamination growth rate. This occurs at a G_{IImax} significantly below the critical strain energy release rate. The reason for this turning point is not presently understood, but it may be speculated that the previous cycles cause a large damage zone ahead of the delamination front, and at a high cyclic G_{IImax}, the delamination propagates through the damage zone at an increased rate.

Other researchers [3,4,28] have used similar methods to characterize mode II cyclic delamination growth of APC-2. A comparison of their mode II fracture toughnesses and exponents B are given in Table 2. As in Table 1, the scatter in results may be from material differences. However, variations in the test method and R ratio used also indicate the need to develop test standards for characterizing mode II delamination.

Comparison of Mode I and Mode II Cyclic Delamination Growth Tests

Figure 6 shows a comparison of the measured mode I and mode II delamination growth rates at the two tested R ratios. For both R ratios the mode I results have steeper slopes than the corresponding mode II results. However, the mode II curves at either R ratio indicate approximately two

orders of magnitude faster delamination growth than the mode I curve at an equivalent G_{max}. This difference is in contradiction to the higher resistance to delamination indicated from the static mode II fracture toughness being higher than the mode I fracture toughness. The result in fig.6 indicates that the resistance to delamination in fatigue is more severly decreased in mode II than in mode I. A possible reason for this difference in delamination growth rates could be the existence of tensile microcracks in the matrix at 45 degrees to the delamination plane, ahead of the delamination front in the ENF test specimen [13]. The delamination growth rate is increased because the failure mode is a coalesence of these microcracks rather than propagation of the delamination through the matrix. Also, in mode I any amount of fiber bridging increases the resistance to fatigue delamination, thus decreasing the delamination growth rate.

For both mode I and mode II tests the delamination growth rates were found to be higher for R=0.1 than for R=0.5 at the same maximum cyclic strain energy release rates. This is true because the applied strain energy release rate range, ΔG, is less at R=0.5 than at R=0.1 even though G_{max} may be the same at the two R ratios.

Threshold Strain Energy Release Rate from Delamination Growth Onset

Mode I Cyclic Delamination Growth Onset

Figure 7 shows the number of cycles to delamination growth onset versus cyclic G_{Imax} for the DCB tests at R=0.1. Several specimens were tested from the insert, i.e., with no pre-crack. As shown in fig.7, the tests run

from the insert had marginally higher number of cycles to delamination growth onset than those run with a shear pre-crack. The threshold value for no delamination growth onset until at least 10^6 cycles at R=0.1 was in the region of 1.0 in-lb/in^2 with no pre-crack and was in the region of 0.7 in-lb/in^2 with a shear pre-crack.

Figure 8 shows the number of cycles to delamination growth onset at R=0.5 for the DCB tests. The figure shows a significant difference between the tests run from the insert and those pre-cracked in shear. Studies by other investigators [29,30] have shown that an R ratio effect does exist, and it was expected that as the R ratio increased the value of G_{th} would also increase. The value of G_{Ith} obtained with a shear pre-crack was in the region of 1.0 in-lb/in^2 at R=0.5. This value obtained from the shear pre-cracked specimens appears to be close to the R=0.1 value of G_{Ith} shown in fig. 7 . However, testing from the insert at R=0.5 indicates that the G_{Ith} value is in the region of 3.0 in-lb/in^2. It appears that the shear pre-cracking masks the effect of the R ratio. As discussed previously, the specimens were pre-cracked to extend the initial delamination tip away from the end of the insert. However, the previously discussed microcracks ahead of the delamination front [13] may cause early delamination growth onset. Thus, the assumption of the structure having no load history had been violated by the pre-cracking procedure. A no load history situation may be more closely approximated by testing at the insert in the DCB. However, because of the relatively thick folded aluminum insert used in these specimens, thresholds measured using delamination growth onset data from the insert may not truly represent the mode I delamination threshold of APC-2.

Further study on the effect of insert thickness is necessary to resolve this problem.

Mode II Cyclic Delamination Growth Onset

The results for the mode II tests at both R=0.1 and R=0.5 are shown in fig. 9. Three specimens were tested from the insert (with no pre-crack) and are shown for comparison. They seem to give a slightly larger number of cycles to delamination growth onset for the same G_{IImax} than the shear pre-cracked specimens. From the results shown in fig. 9, the threshold values for no delamination growth onset until at least 10^6 cycles are 0.7 in-lb/in^2 at R=0.1 and 1.0 in-lb/in^2 at R=0.5. As in the DCB specimens the shear pre-cracking caused damage in the form of tensile microcracks ahead of the delamination front. Therefore, pre-cracked specimens are not truly representative of a no load-history situation and may give unnecessarily conservative threshold values. Further investigations with and without pre-cracks, and using a variety of insert thicknesses, are necessary to determine the optimum specimen configuration to find the threshold strain energy release rate for no delamination growth onset.

Comparison of Mode I and Mode II results

Figures 7, 8 and 9 show that strain energy release rate thresholds for both mode I and mode II loadings at R ratios of R=0.1 and R=0.5 show a marked decrease from the static fracture toughness for both pre-cracked and

no pre-crack specimens. This indicates that the increase in resistance to delamination achieved by thermoplastics under static loads is significantly reduced under cyclic loads.

Comparison of mode I and mode II delamination growth onset curves are shown in figs. 10 and 11 for R=0.1 and R=0.5 respectively with specimens that were pre-cracked in shear. Comparisons of specimens that were pre-cracked in shear were made because similar damage caused by the pre-cracking process existed ahead of the delamination front in both the DCB and ENF test specimens. The data points for mode I and mode II indicate that G_{Ith} and G_{IIth} are similar for either R ratio. O'Brien et al [13] compared the maximum cyclic strain energy release rate as a function of cycles to delamination onset for AS4/PEEK and T300/BP907 in pure mode II and a mixed mode Edge Delamination Test, EDT, specimen. For both materials the mode II and mixed-mode curves were coincident for tests at R=0.1 and thus the pure mode II threshold and the mixed-mode threshold were similar. They therefore hypothesized that only the total strain energy release rate threshold need be considered to predict cyclic delamination behavior. The similar mode I and mode II threshold values shown in figs. 10 and 11 agree with the hypothesis of reference 13. However, further delamination growth onset tests on APC-2 mixed-mode specimens are necessary to verify if there are any mixed-mode synergistic effects.

Comparison of Delamination Growth Arrest and No Delamination Growth Onset

At R=0.1 the DCB becomes largely unloaded at the minimum displacement in the fatigue cycle. As the fatigue test progresses the amount of facial interference increases throughout the fatigue cycle and the length of time

that the delamination tip is open is greatly reduced. Fig.4 shows at R=0.1 the delamination growth did arrest at G_{Imax} =3.0 in-lb/in^2. Comparison of this value of G_{Imax} with the value of G_{Ith} obtained from delamination growth onset tests at R=0.1, i.e. G_{Ith} = 0.7 in-lb/in^2 shows a significant difference in the two methods used to obtain a threshold value. It should be concluded that G_{th} values measured from tests to delamination growth onset are more conservative than values measured using delamination growth arrest.

FULL FATIGUE CHARACTERIZATION OF COMPOSITE MATERIALS

Finally, to the authors' knowledge, there is no expression that expresses the delamination growth rate in terms of the maximum cyclic strain energy release rate, the threshold strain energy release rate and the static fracture toughness. Such a relationship would be useful for a full characterization of the fatigue delamination behavior of a composite material. Therefore, the following power law expression for the delamination growth rate was postulated:

$$\frac{da}{dN} = A\,(G_{max})^{B}\,\frac{[1-(G_{th}/G_{max})^{D_1}]}{[1-(G_{max}/G_{c})^{D_2}]} \qquad (9)$$

which applies between the limits $G_{th} \leq G_{max} \leq G_c$. Therefore, from equation (9), as G_{max} tends towards G_{th}, da/dN tends towards zero. Also, as

G_{max} tends towards G_c, da/dN tends towards infinity. Between the limits of G_{th} and G_c the predominant term in equation (9) is $A\,(G_{max})^B$.

The constants A and B in equation (9) may be found from the cyclic delamination growth tests described previously. The threshold strain energy release rate, G_{th}, may be found from tests of no delamination growth onset until at least 10^6 cycles. The term G_c is the fracture toughness. The constants D_1 and D_2 can be found by fitting equation (9) to the experimental data.

Figure 12 shows how equation (9) could theoretically be used to evaluate the exponents D_1 and D_2 using the results for mode II testing at R=0.1. However, several reservations must be noted to viewing equation (9) as a unifying law for delamination characterization. Several precautions are necessary to accurately determine the constants D_1 and D_2. For the DCB, fig. 4 showed sufficient data points at the lower turning point for mode I testing at R=0.1. However, the use of equation (9) in this example may be misleading since as this turning point is not at a threshold value of G_{Imax} as described above. Therefore, determination of the constant D_1 by fitting experimental data at R=0.1 for mode I testing may be inaccurate. For the ENF test, in fig. 5, at both R ratios used, the turning point between cyclic delamination growth and static fracture toughness occurred at a G_{IImax} significantly below G_{IIc}. Therefore, determination of the constant D_2 by fitting experimental data for mode II may be inaccurate.

CONCLUSIONS

Cyclic Double Cantilever Beam (DCB) and End-notched Flexure (ENF) tests were conducted on APC-2, AS4/PEEK. Tests were run at a frequency of 5 Hz, at two different displacement ratios, R=0.1 and R=0.5. Delamination growth rates and corresponding strain energy release rates were measured, and the number of cycles to delamination growth onset were recorded. A power law relating delamination growth to cyclic strain energy release rate was found. A threshold strain energy release rate was chosen to correspond to no delamination growth onset until at least 10^6 cycles. From the results of these tests the following conclusions were drawn:

1. The mode II delamination growth rate is approximately two orders of magnitude faster than the mode I delamination growth rate at equivalent values of G_{max} and R ratio. This difference is because of the lower resistance to fatigue delamination in mode II than in mode I, possibly caused by microcracks in the matrix ahead of the delamination in the ENF and fiber bridging in the DCB. For the same G_{max} the delamination growth rates for mode I and mode II at R=0.5 are slower than at R=0.1 because the amplitude of the cyclic strain energy release rate is greater at R=0.1 than at R=0.5.

2. In the DCB, a higher number of cycles to delamination growth onset was obtained when the delamination grew from an aluminum insert rather than at a static load induced shear pre-crack. The difference in the number of cycles to delamination growth onset was noticeably larger at R=0.5

than at R=0.1. This variation may be caused by damage occurring ahead of the delamination front during the pre-cracking procedure, thus allowing delamination growth onset at a lower number of cycles than at an insert where there is no damage.

3. A large difference was observed between G_{th} and G_c for both modes and for both R ratios used in this study. This difference indicates that the increased resistance to delamination achieved by thermoplastics under static loads is significantly reduced under cyclic loads.

4. The values of G_{Ith} and G_{IIth} determined from delamination growth onset tests were similar for displacement ratios of R=0.1 and R=0.5. Comparisons of DCB and ENF specimens that had been statically pre-cracked were made because similar damage existed ahead of the delamination front. Therefore, if a linear fatigue criterion is assumed, then a total G threshold criterion appears to be sufficient for characterizing delamination of structures with mixed-mode delaminations that are subjected to cyclic loadings.

5. Delamination arrest occurred in the DCB at R=0.1 at a G_{Imax} of 3 in-lb/in^2. This G_{Imax} value at delamination arrest was significantly higher than the value of G_{Ith}=0.7 in-lb/in^2 obtained by delamination growth onset tests. The delamination growth arrest value of G_{Imax} was larger because facial interference (consisting of fiber bridging, a plasticity zone wake, surface roughness and debris) acted to

artificially close the delamination tip throughout part of the fatigue cycle, thus causing delamination arrest.

6. Finally, a power law expression was postulated that relates delamination growth rate to both the threshold strain energy release rate and the static fracture toughness.

ACKNOWLEDGEMENTS

This work was done while the first author held a National Research Council-NASA Langley Research Associateship. The authors wish to acknowledge the technical assistance of Dr. T.K. O'Brien of the U.S. Army Aerostructures Directorate.

REFERENCES

1. Carlile, D.R. and Leach, D.C.,"Damage and Notch Sensitivity of Graphite/PEEK Composites," Proceedings of the 15th National SAMPE Technical Conference, October 1983, pp. 82-93.

2. Ramkumar, R.L. and Whitcomb, J.D., "Characterization of Mode I and Mixed Mode Delamination Growth in T300/5208 Graphite/Epoxy," Delamination and Debonding of Materials, ASTM STP 876, W.S.Johnson Ed., 1985, pp 315-335.

3. Mall, S., Yun, K.T., and Kochhar, N.K., "Characterization of Matrix Toughness Effect on Cyclic Delamination Growth in Graphite Fiber Composites," Presented at the 2nd ASTM Symposium on Composite Materials: Fatigue and Fracture, Cincinnati, Ohio, April 1987.

4. Prel, Y.J., Davies, P., Benzeggagh, M.L., and de Charentenay, Fx., "Mode I and Mode II Delamination of Thermosetting and Thermoplastic Composites," Presented at the 2nd ASTM Symposium on Composite Materials: Fatigue and Fracture, Cincinnati, Ohio, April 1987.

5. de Charentenay, F.X., Harry, J.M., Prel, Y.J. and Benzeggagh, M.L., "Characterizing the Effect of Delamination Defect by Mode I Delamination Test," Effect of Defects in Composite Materials, ASTM STP 836, 1984, pp.84-103

12. O'Brien, T.K., "Towards a Damage Tolerance Philosophy for Composite Materials and Structures," To be presented at the 9th ASTM Symposium on Composite Materials: Testing and Design, Reno, Nevada, April 1988.

13. O'Brien, T.K., Murri, G.B., and Salpekar, S.A., "Interlaminar Shear Fracture Toughness and Fatigue Thresholds for Composite Materials," NASA TM 89157, August 1987, Presented at the 2nd ASTM Symposium on Composite Materials: Fatigue and Fracture, Cincinnati, OH, April 1987.

14. Wakelyn, N.T., "Resolution of Wide Angle X-ray Scattering from a Thermoplastic Composite," Journal of Polymer Science: Part A: Polymer Chemistry, Vol. 11, 1977, p.470.

15. Murri, G.B. and O'Brien, T.K., "Interlaminar G_{IIc} Evaluation of Toughened Resin Matrix Composites Using the End-Notched Flexure Test," AIAA-85-0647, Proceedings of the 26th AIAA/ASME/ASCE/AHS Conference on Structures, Structural Dynamics and Materials, Orlando, Florida, April, 1985, p197.

16. Russell, A.J., "Factors Affecting the Opening Mode Delamination of Graphite/Epoxy Laminates," Defence Research Establishment Pacific (DREP), Canada, Materials Report 82-Q, December 1982.

17. Johnson, W.S. and Mangalgiri, P.D., "Investigation of Fiber Bridging in Double Cantilever Beam Specimens," Journal of Composites Technology and Research, Vol.9, No.1, Spring 1987, pp. 10-13.

6. Russell, A.J. and Street, K.N., "The Effect on Matrix Toughness on Delamination: Static and Fatigue Fracture Under Mode II Shear Loading of Graphite Fiber Composites," Toughened Composites, ASTM STP 937, N.J.Johnston, Ed., 1987, pp. 275-294

7. Carlile, D.R., Leach, D.C., Moore, D.R. and Zahlan, N., "Mechanical Properties of PEEK/ Carbon Fiber Composites (APC-2) for Structural Applications," presented at the ASTM symposium on Advances in Thermoplastic Matrix Composite Materials, Bal Harbour, Florida, October 1981.

8. Clark, W.G. Jr. and Hudak, S.J. Jr., "Variability in Fatigue Crack Growth Rate Testing," Journal of Testing and Evaluation, Vol. 3, No. 6, 1975, pp. 454-476.

9. Fatigue Thresholds, Fundamentals and Engineering Applications, Vol. I and II, Engineering Materials Advisory Services Ltd., Eds. Backlund, J., Blom, A.F. and Beevers, C.J., 1982.

10. Johnson, W.S. and Mall, S., "A Fracture Mechanics Approach for Designing Adhesively Bonded Joints," Delamination and Debonding of Materials, ASTM STP 876, W.S. Johnson Ed., 1985, pp. 189-199.

11. O'Brien, T.K., "Generic Aspects of Delamination in Fatigue of Composite Materials," Journal of the American Helicopter Society, Vol. 32, No. 1, January 1987, pp. 13-18.

18. Whitcomb, J.D., "A Simple Calculation of Strain Energy Release Rate for a Nonlinear Double Cantilever Beam," Journal of Composites Technology and Research, Vol.7, No.2, Summer 1985, pp. 64-66.

19. Williams, J.G., "Large Displacement and End Block Effects in the DCB Interlaminar Test in Modes I and II," Journal of Composite Materials, Vol.21, April 1987, pp. 330-347.

20. Gillespie, J.W. Jr., Carlsson, L.A. and Smiley, A.J., "Rate Dependent Mode I Interlaminar Crack Growth Mechanisms in Graphite Epoxy and Graphite/PEEK," Composites Science and Technology, Vol. 28, 1987, pp. 1-5.

21. Smiley, A.J. and Pipes, R.B., "Rate Effects on Mode I Interlaminar Fracture Toughness in Composite Materials," Journal of Composite Materials, Vol.21, July 1987, pp. 670-687.

22. Mall, S., Law, G.E. and Katouzian, M., "Loading Rate Effects on Interlaminar Fracture Toughness of a Thermoplastic Composite," Journal of Composite Materials, Vol.21, June 1987, pp. 569-579.

23. Schapery, R.A., Goetz, D.P. and Jordan, W.M., "Delamination Analysis of Composites with Distributed Damage Using a J Integral," Proceedings of the International Symposium on Composite Materials and Structures, Beijing, China, June 1986, Technomic Publishing Co., pp.543-548.

24. Keary, P.E., Ilcewicz, L.B., Shaar, C. and Trostle, J., "Mode I Interlaminar Fracture Toughness of Composite Materials Using Slender Double Cantilever Beam Specimens," Journal of Composite Materials, Vol.19, March 1985, pp. 154-177.

25. Carlsson, L.A., and Byron Pipes, R., Experimental Characterization of Advanced Composite Materials, Prentice-Hall Inc., New Jersey 1987.

26. Whitney, J.M., Browning, C.E. and Hoogsteden, W., "A Double Cantilever Beam Test for Characterizing Mode I Delamination of Composite Materials," Journal of Reinforced Plastics and Composites, Vol.1, October 1982, pp.297-313.

27. Russell, A.J., "On the measurement of Mode II Interlaminar Fracture Energies," Defence Research Establishment Pacific (DREP), Canada, Materials Report 82-0, December 1982.

28. Russell, A.J., and Street, K.N., "Predicting Interlaminar Fatigue Crack Growth Rates in Compressively Loaded Laminates," Presented at the 2nd ASTM Symposium on Composite Materials: Fatigue and Fracture, Cincinnati, Ohio, April 1987.

29. Bathias, C. and Laksimi, A., "Delamination Threshold and Loading Effect in Fiberglass Epoxy Composite," Delamination and Debonding of Materials, ASTM STP 876, W.S.Johnson, Ed., 1985, pp. 217-237.

30. Adams, D.F., Zimmerman, R.S. and Odom, E.M., "Frequency and Load Ratio Effects on Critical Strain Energy Release Rate G_c Thresholds of Graphite Epoxy Composites," in Toughened Composites, ASTM STP 937, N.J.Johnston Ed., 1987, pp. 242-259.

Table 1. Comparison of Exponent B and Fracture Toughness for Mode I Testing of AS4/PEEK in Literature

REFERENCE	EXPONENT B	G_{Ic} (in-lb/in^2)	
		Initiation	Propagation
Current Study	6.14	-	9.7-14.1[a]
Mall, Yun and Kochhar, 1987, [3]	4.8	-	6.9
Prel, Davies, Benzeggagh and de Charentenay, 1987, [4]	10.5	8.3	13.7
Russell and Street, 1987, [6-28]	3.0	7.6	8.8

where B is the exponent in the power law $da/dN = A\ G_I^B$

All results are at R=0.1

- - Not available

a - From ASTM Round Robin

Table 2. Comparison of Exponent B and Fracture Toughness for Mode II Testing of AS4/PEEK in Literature

REFERENCE	MODE II TEST	R	EXPONENT B	G_{IIc} (in-lb/in^2)
Current Study	ENF	0.1	3.64	14.2-21.5[a]
	ENF	0.5	5.34	14.2-21.5[a]
Mall, Yun and Kochhar, 1987, [3]	ENF	0.1	3.66	8.6
Prel, Davies, Benzeggagh and de Charentenay, 1987, [4]	CBEN	-1	2.0[b]	10.6-15.4
Russell and Street, 1987, [28]	ENCB	-1	2.02	8.7-11.4
	ENCB	0	3.88	8.7-11.4

where B is the exponent in the power law $da/dN = A\ (G_{II})^B$

a - from ASTM Round Robin

b - Approximate value determined from figure 10 in reference 4.

FIGURE CAPTIONS

Figure 1 Diagram of DCB Specimen

Figure 2 Diagram of ENF Specimen

Figure 3 ENF Test Set Up

Figure 4 Mode I Fatigue Delamination Growth Rates

Figure 5 Mode II Fatigue Delamination Growth Rates

Figure 6 Comparison of Mode I and Mode II Delamination Growth Rates

Figure 7 Mode I Delamination Growth Onset at R=0.1

Figure 8 Mode I Delamination Growth Onset at R=0.5

Figure 9 Mode II Delamination Growth Onset at R=0.1 and R=0.5

Figure 10 Comparison of Mode I and Mode II Delamination Growth Onset at R=0.1

Figure 11 Comparison of Mode I and Mode II Delamination Growth Onset at R=0.5

Figure 12 Delamination Power Law Fitted to Experimental Data

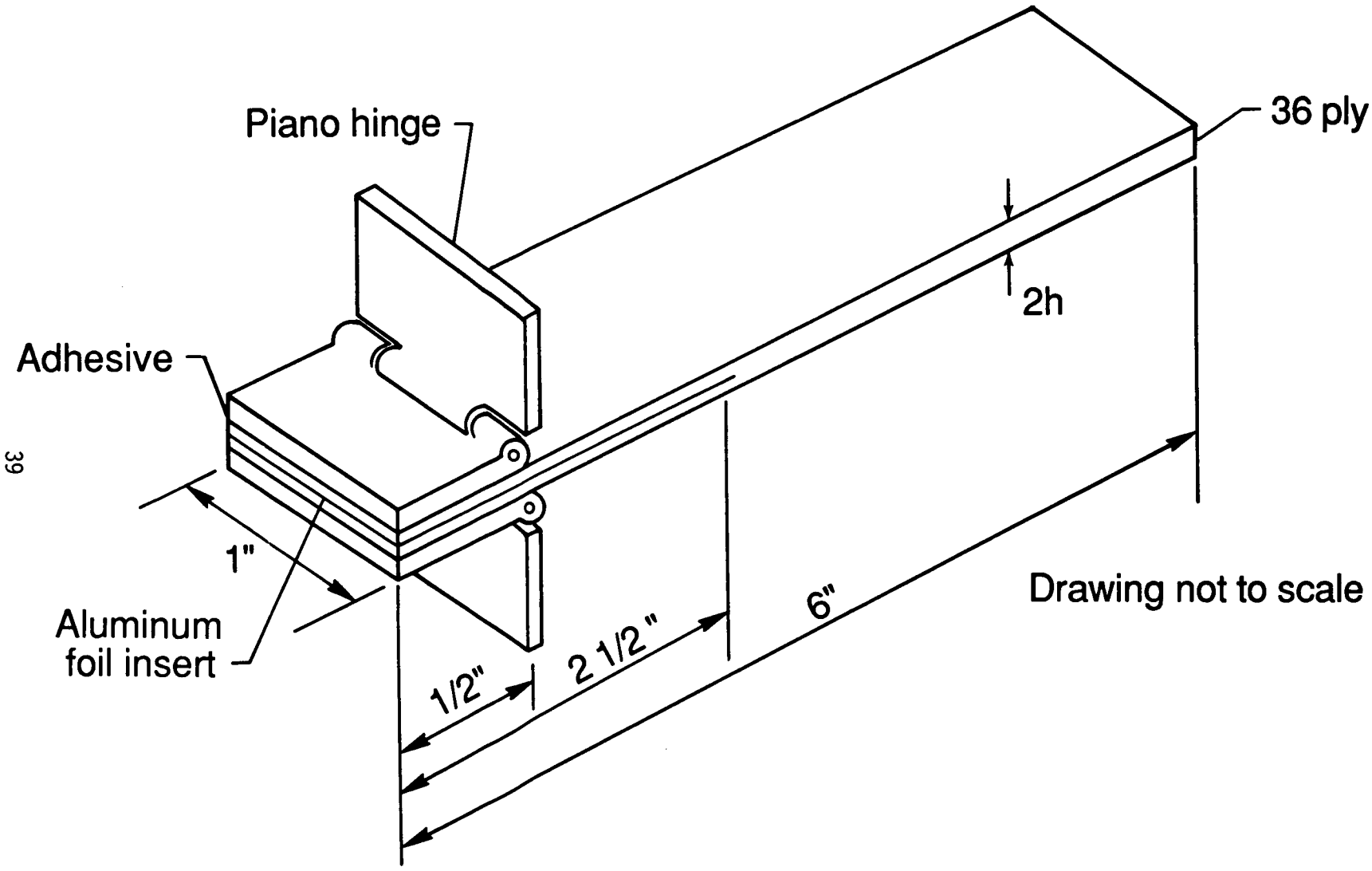

Figure 1. - Diagram of DCB specimen.

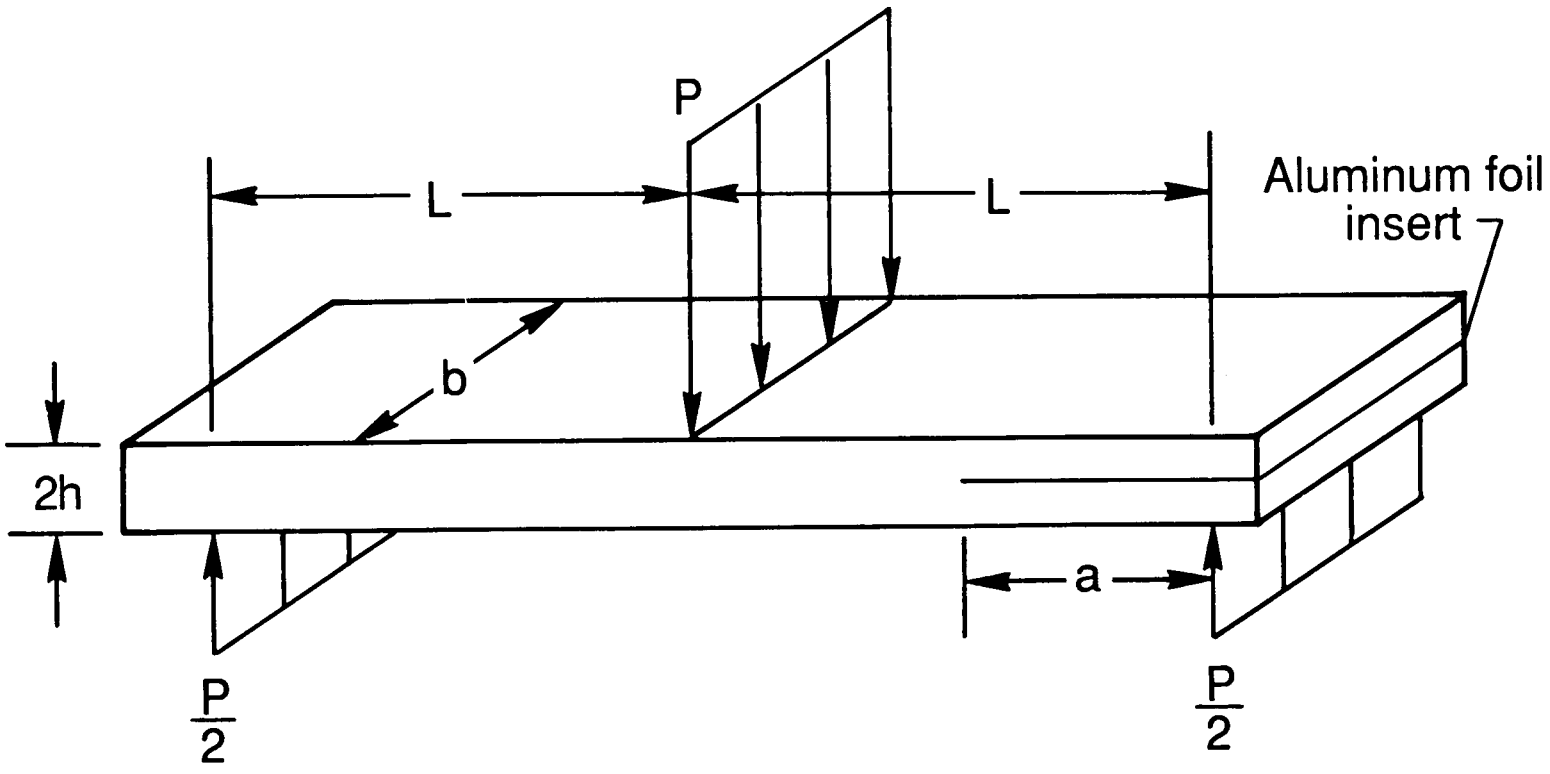

Figure 2. - Diagram of ENF specimen.

Figure 3. - ENF test set up.

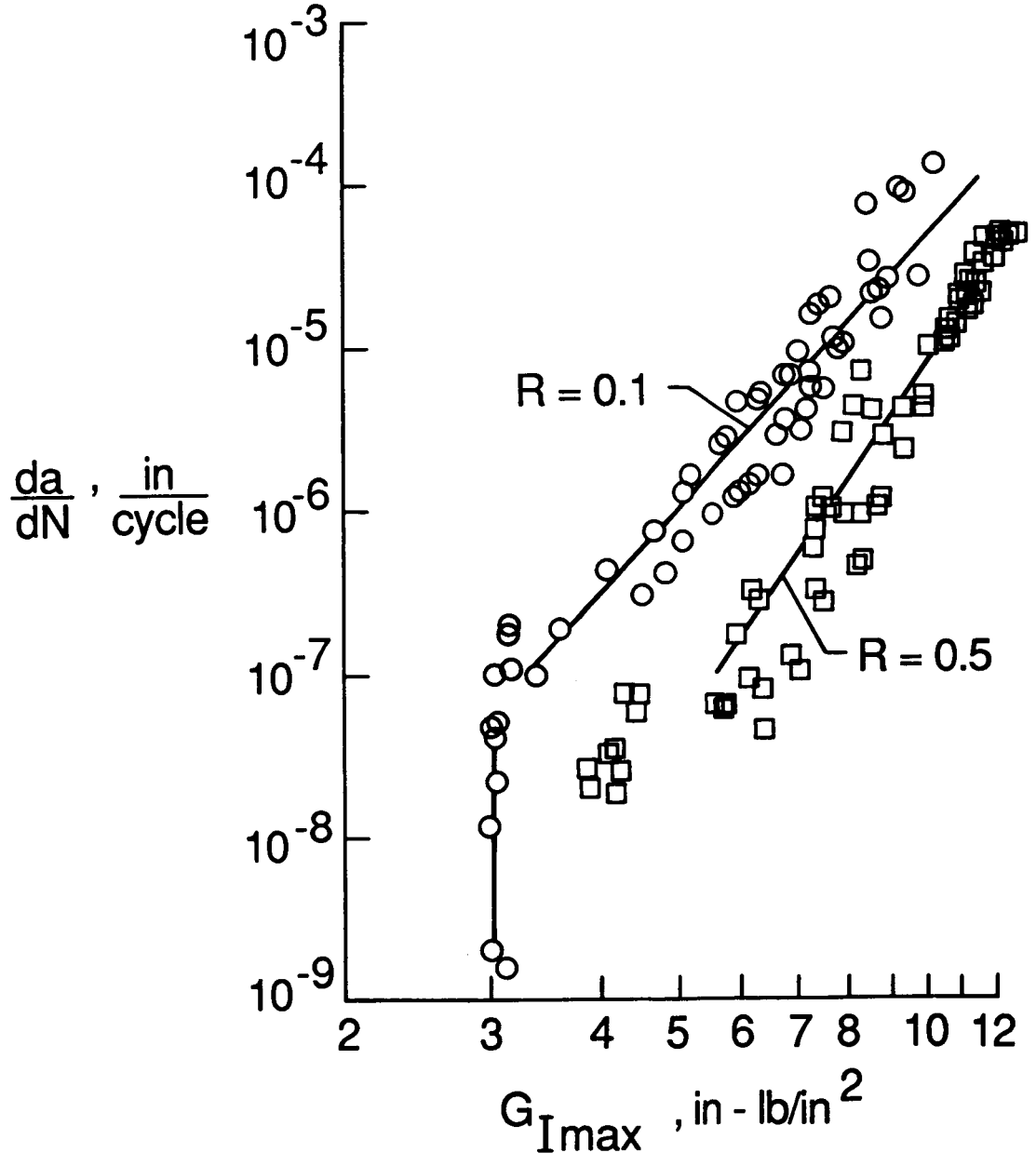

Figure 4. - Mode I fatigue delamination growth rates.

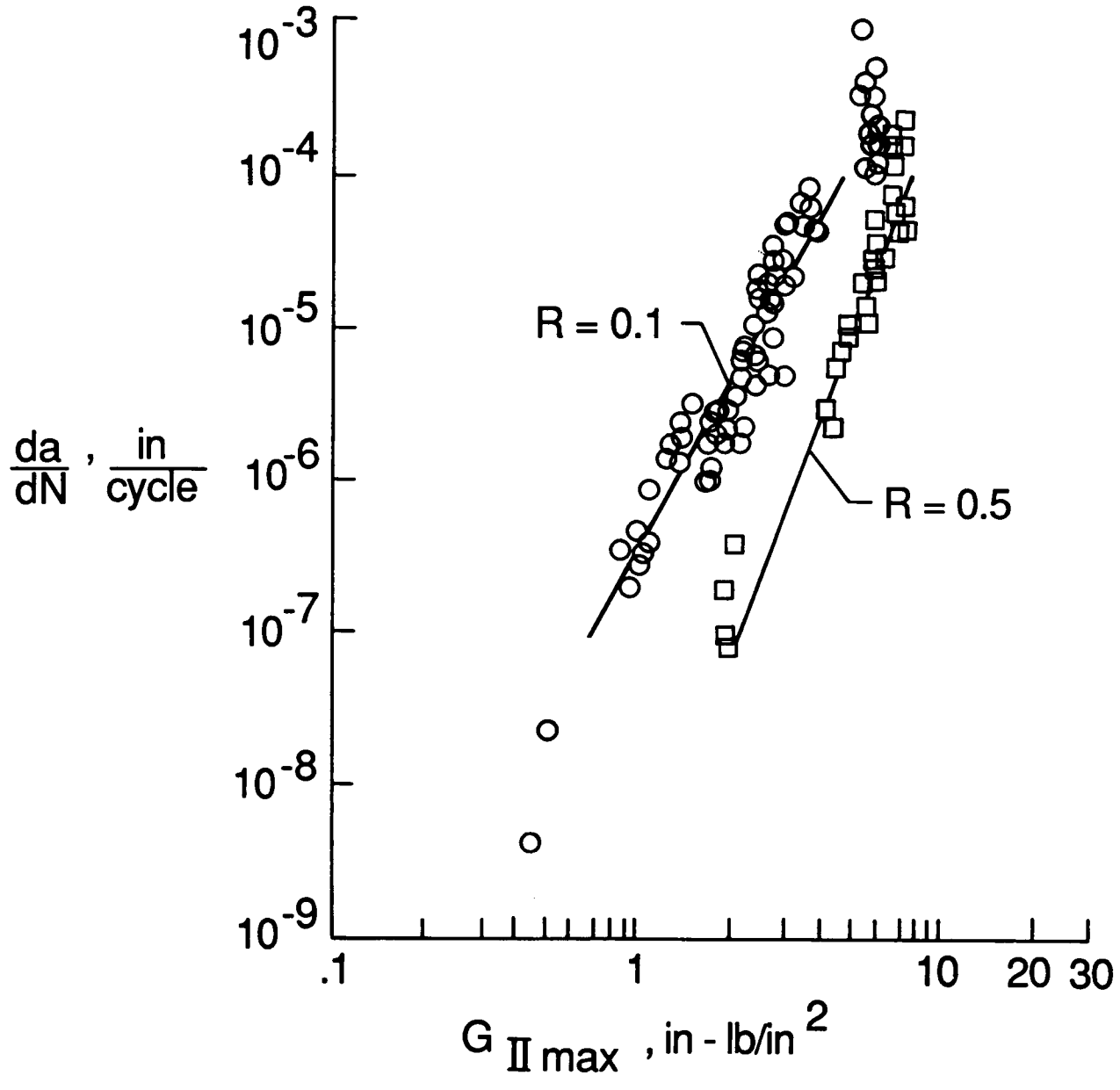

Figure 5. - Mode II fatigue delamination growth rates.

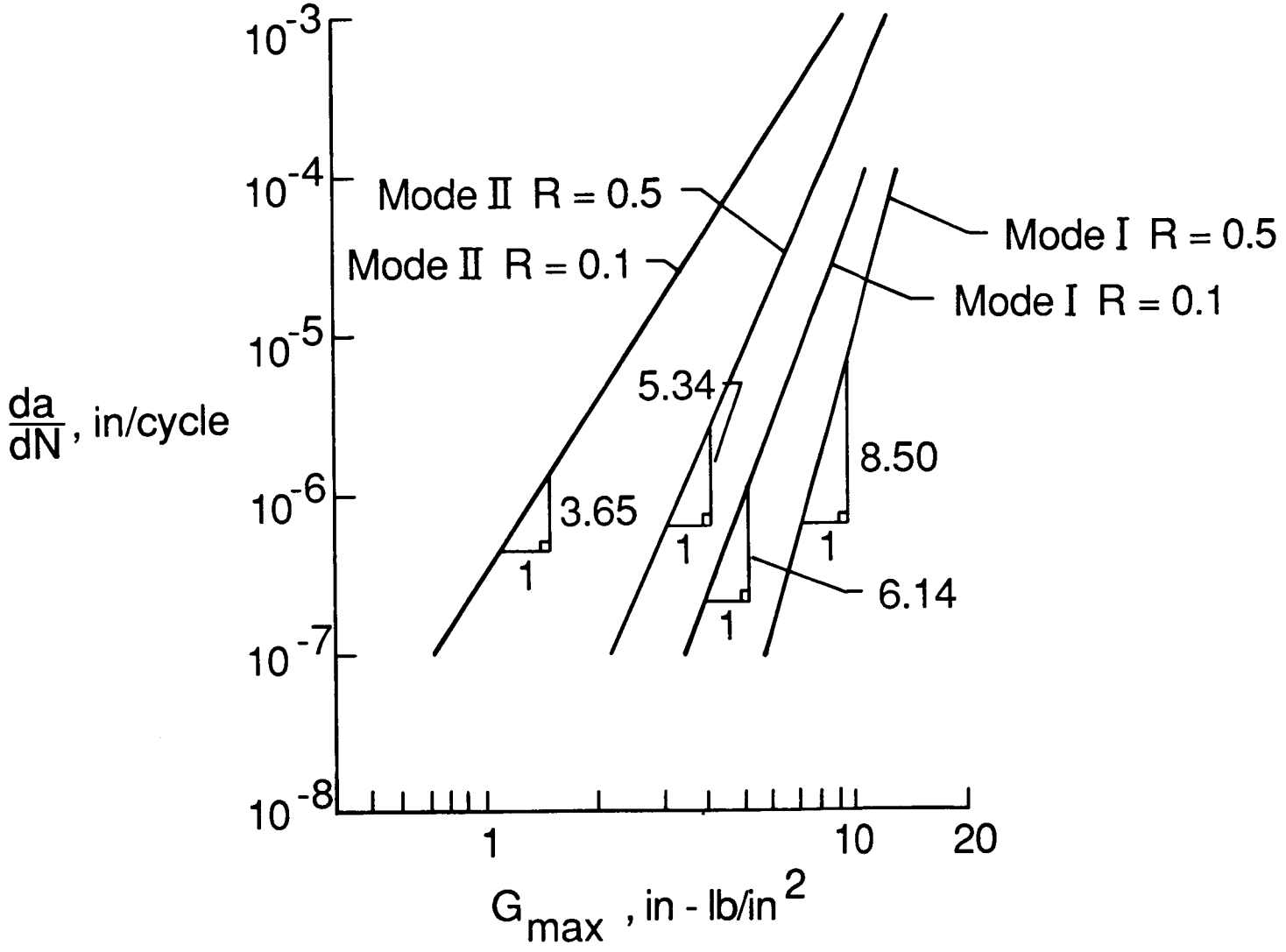

Figure 6. - Comparison of mode I and mode II delamination growth rates.

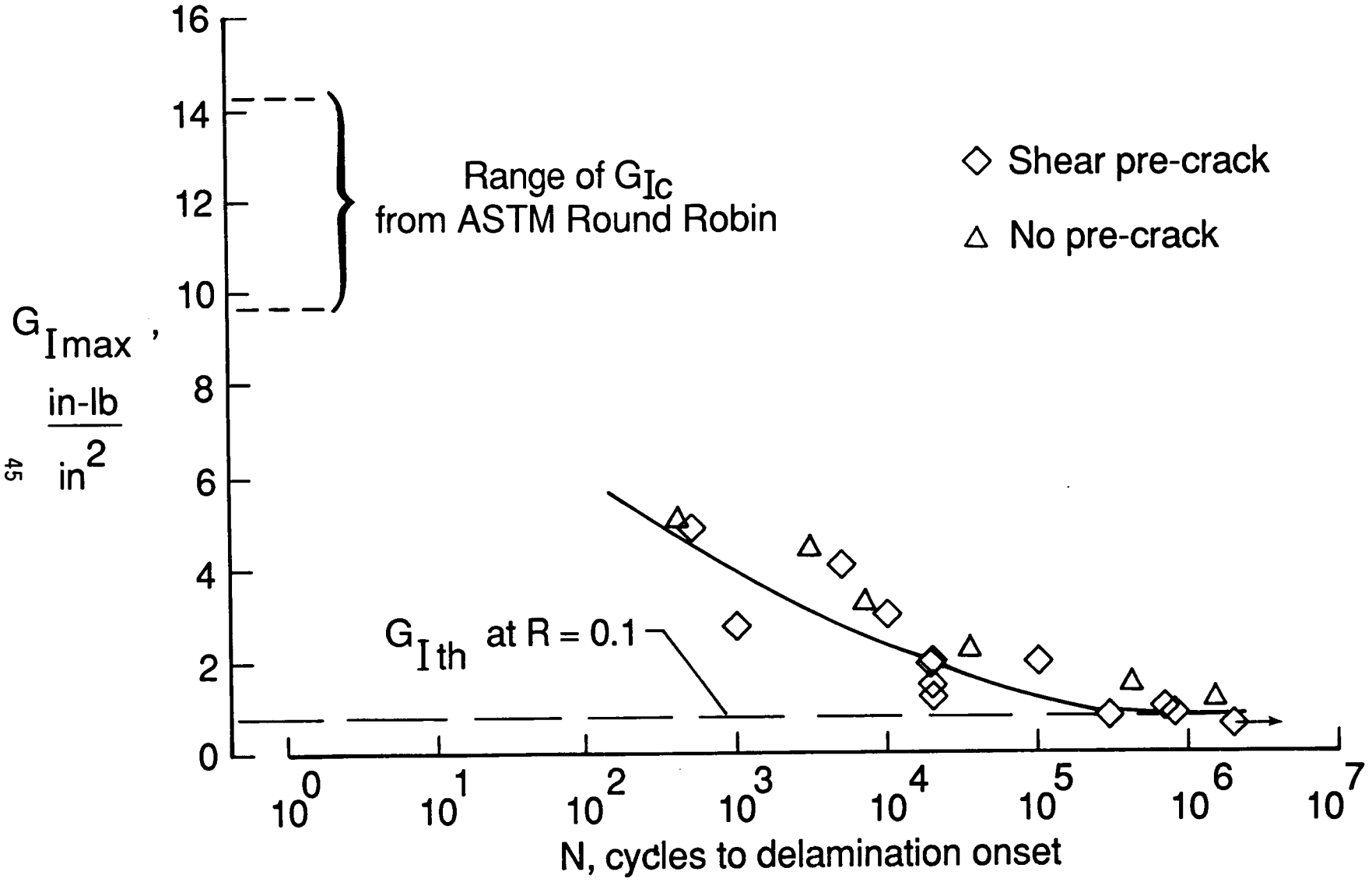

Figure 7. - Mode I delamination growth onset at R=0.1.

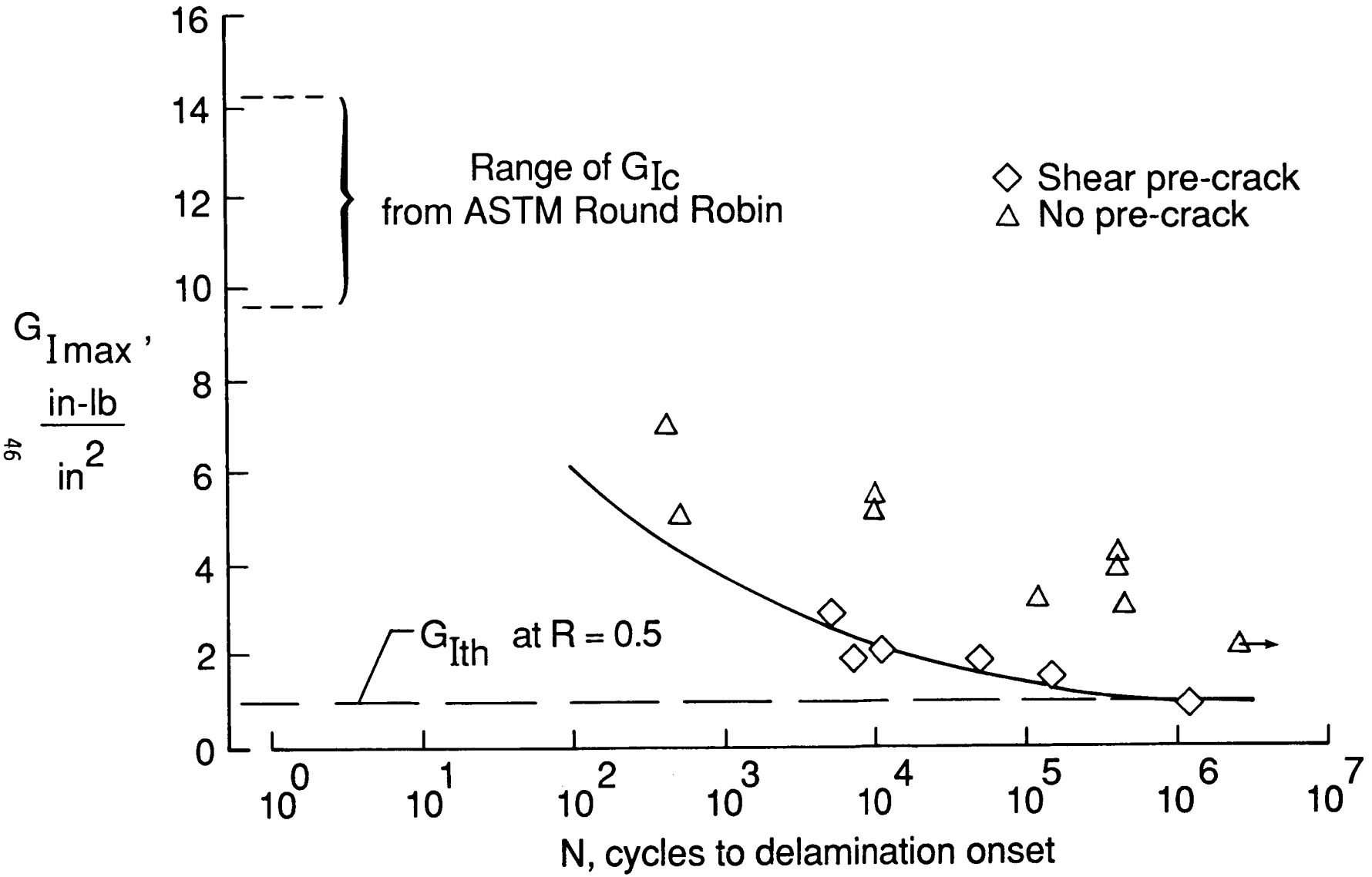

Figure 8. - Mode I delamination growth onset at R=0.5.

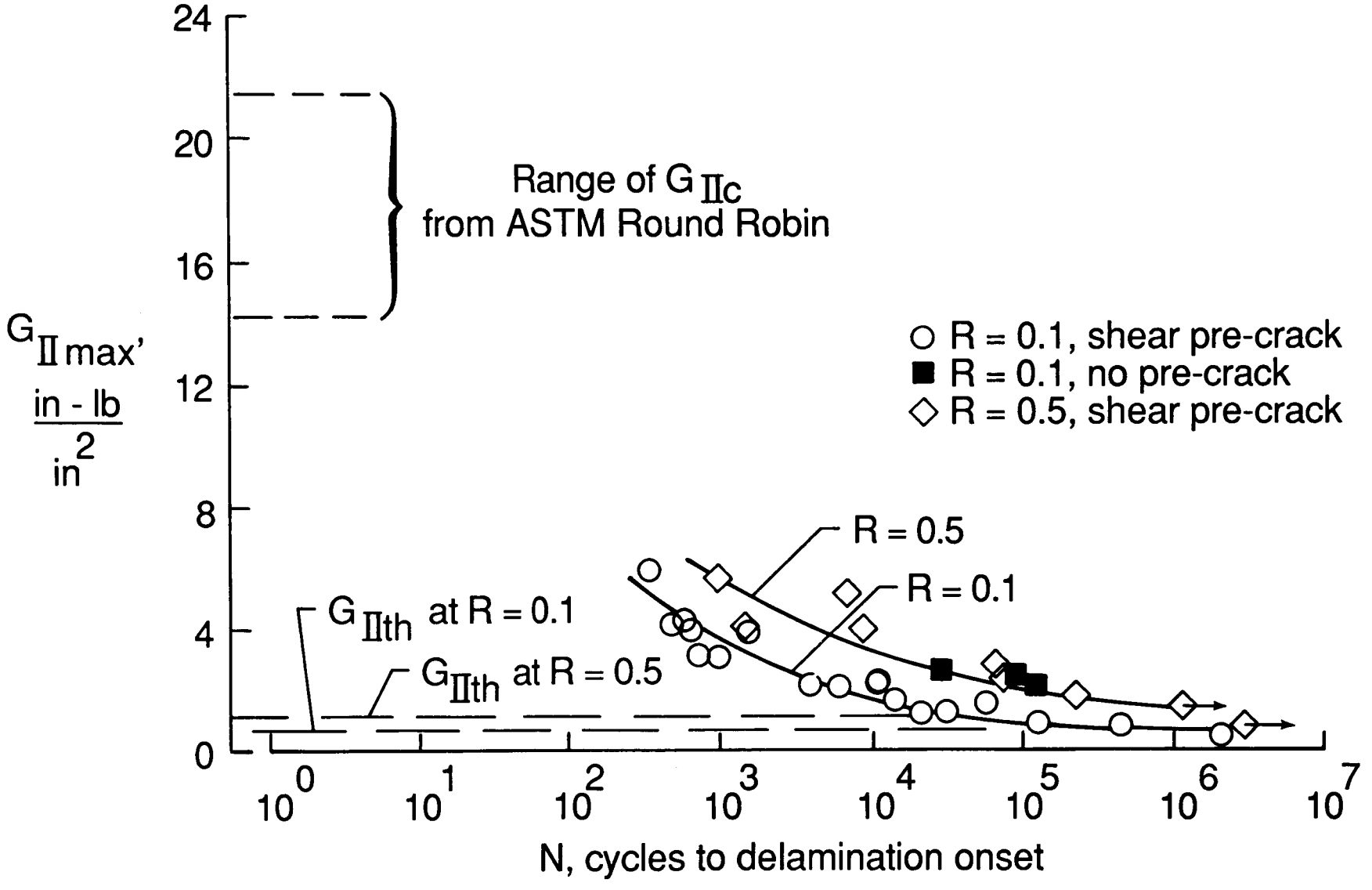

Figure 9. - Mode II delamination growth onset at R=0.1 and R=0.5.

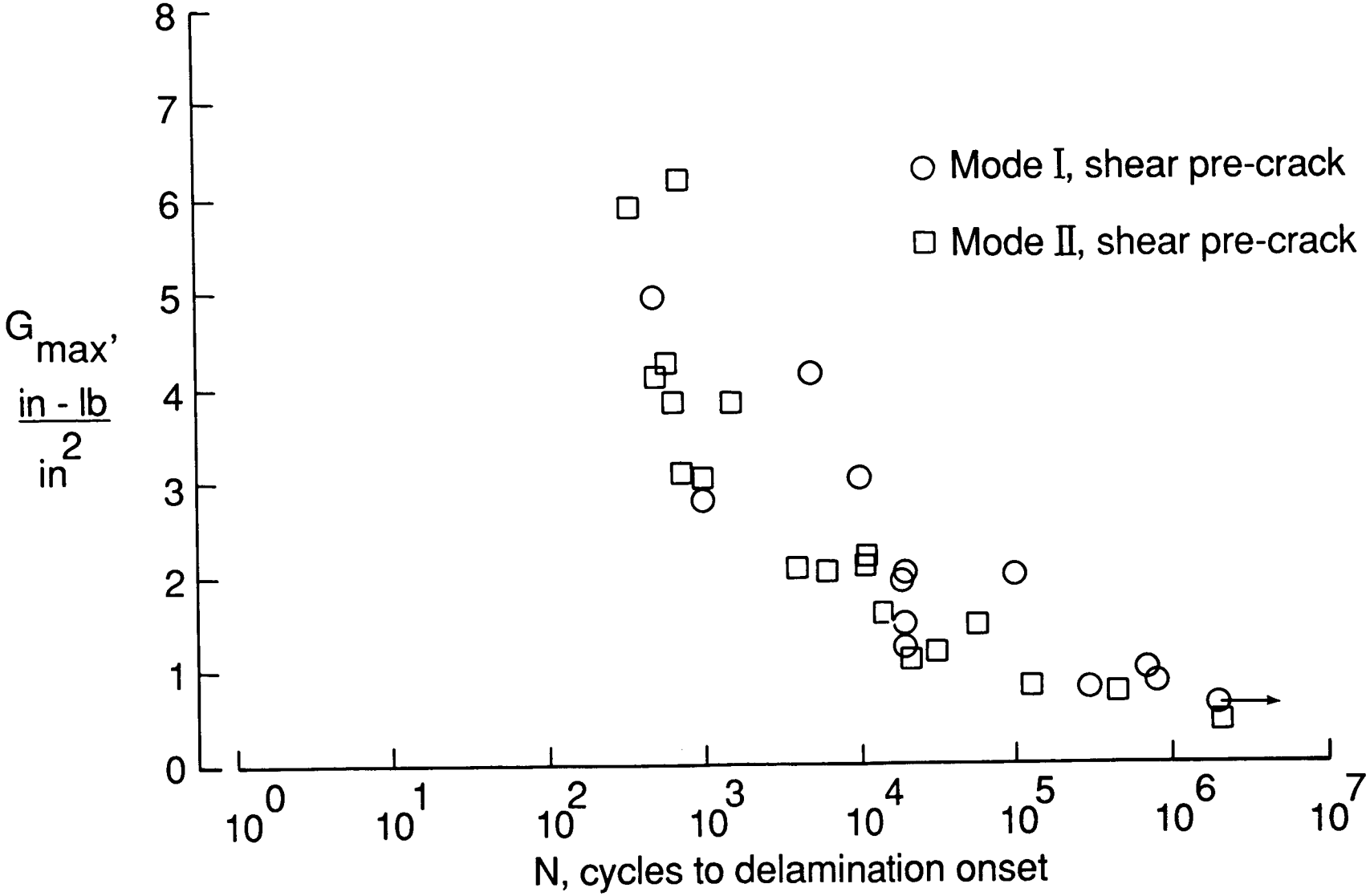

Figure 10. - Comparison of mode I and mode II delamination growth onset at R=0.1.

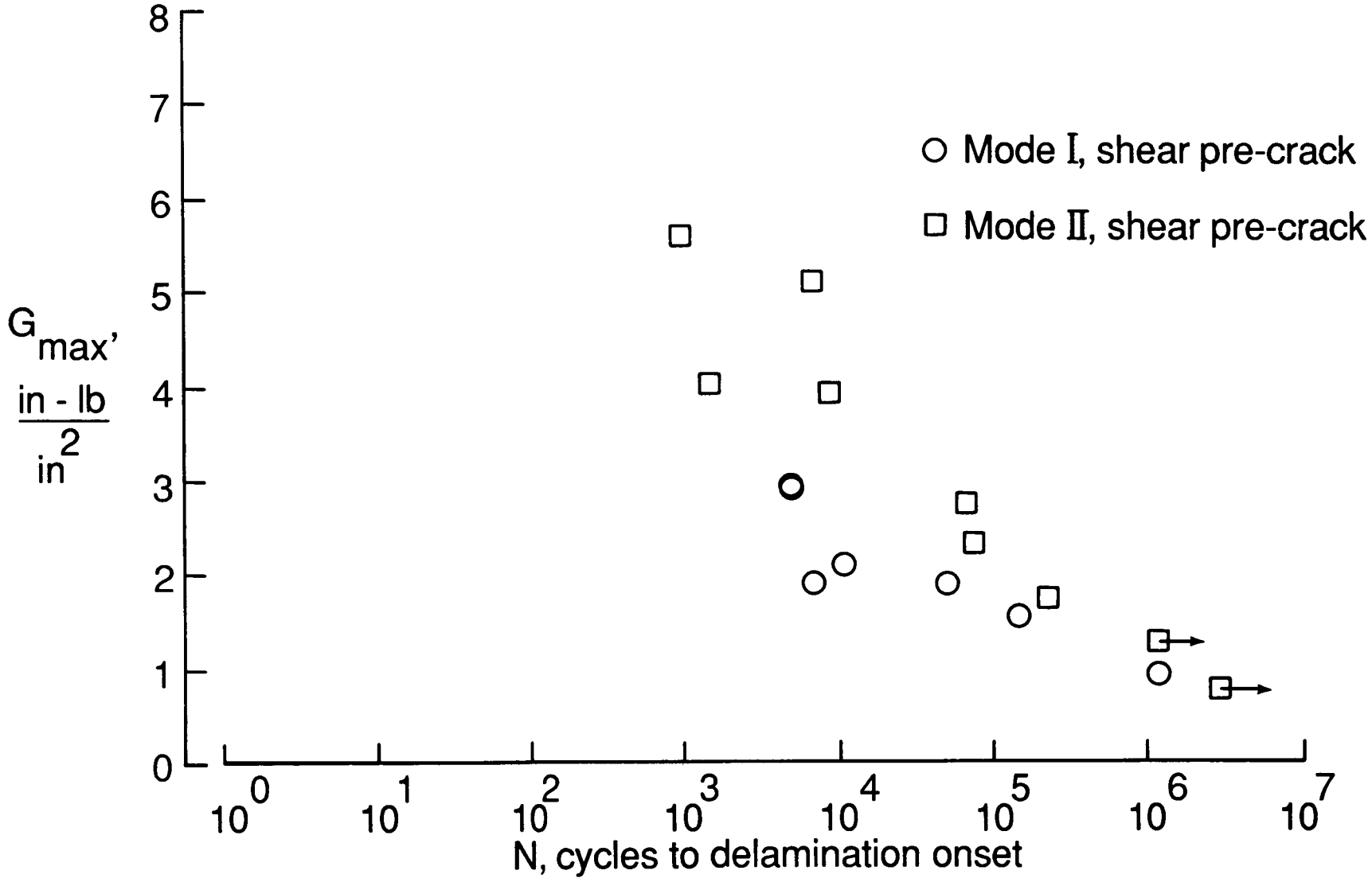

Figure 11. - Comparison of mode I and mode II delamination growth onset at R=0.5.

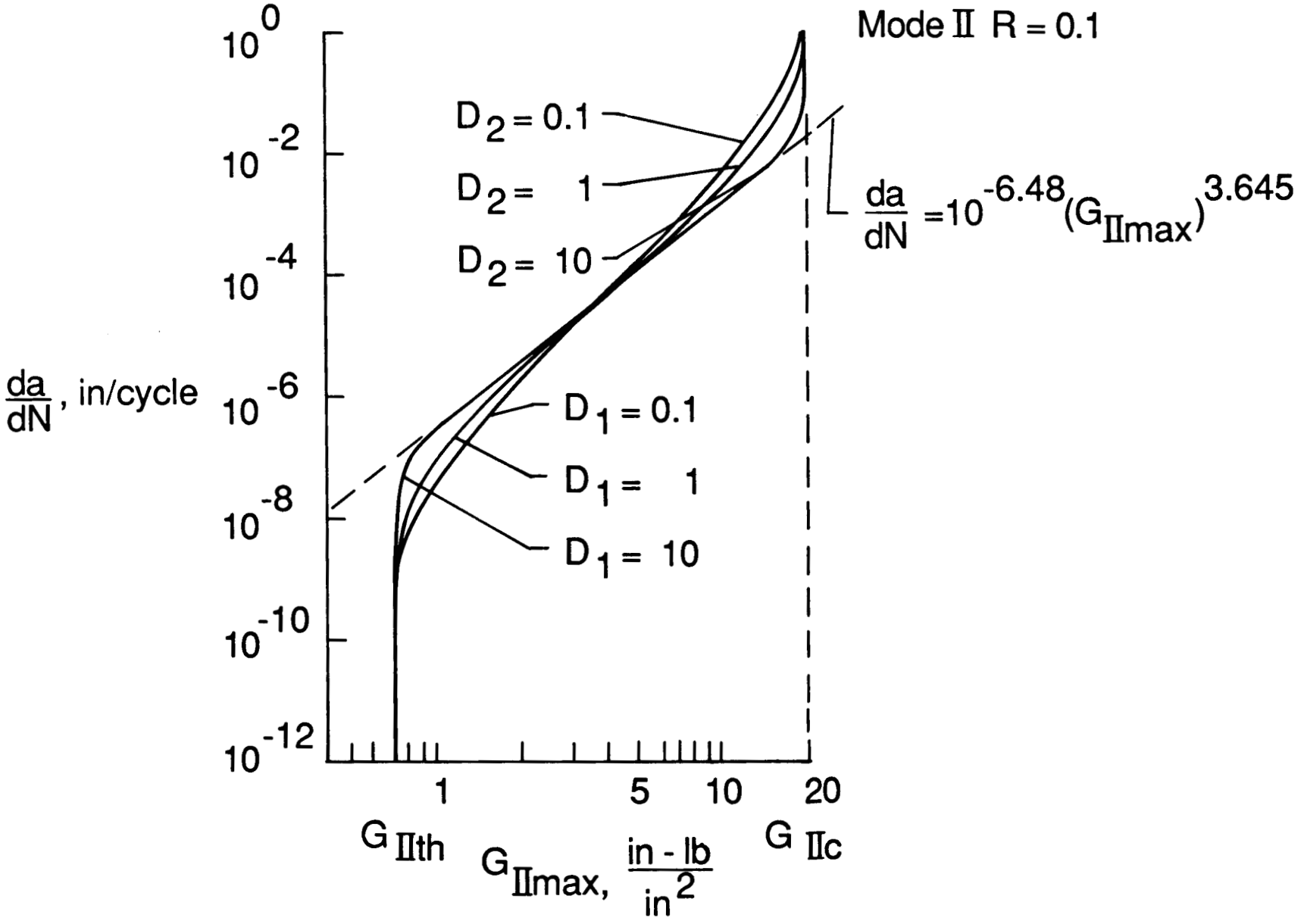

Figure 12. - Delamination power law fitted to experimental data.

1. Report No. NASA TM-100577	2. Government Accession No. AVSCOM TM 88-B-011	3. Recipient's Catalog No.

4. Title and Subtitle
Characterization of Mode I and Mode II Delamination Growth and Thresholds in Graphite/Peek Composites

5. Report Date
April 1988

6. Performing Organization Code

7. Author(s)
Roderick H. Martin and Gretchen B. Murri

8. Performing Organization Report No.

9. Performing Organization Name and Address
NASA Langley Research Center, Hampton, VA 23665-5225
U.S. Army Aviation Research and Technology Activity (AVSCOM)
Aerostructures Directorate
Hampton, VA 23665-5225

10. Work Unit No.
505-63-01-05

11. Contract or Grant No.

12. Sponsoring Agency Name and Address
National Aeronautics and Space Administration
Washington, DC 20546

U.S. Army Aviation Systems Command
St. Louis, MO 63166

13. Type of Report and Period Covered
Technical Memorandum

14. Army Project No.
1L161102AH45C

15. Supplementary Notes

Roderick H. Martin, National Research Council (NRC) Resident Research Associate
Gratchen B. Murri, Aerostructures Directorate, USAARTA-AVSCOM, Langley Res. Center

16. Abstract
Composite materials often fail by delamination and, their delamination behavior needs to be fully characterized. In this paper the onset and growth of delamination in AS4/PEEK, a tough thermoplastic matrix composite, was characterized for mode I and mode II loadings, using the Double Cantilever Beam (DCB) and the End-notched Flexure (ENF) test specimens, respectively. Delamination growth per fatigue cycle, da/dN, was related to strain energy release rate, G, by means of a power law. However, the exponents of these power laws were too large for them to be adequately used as a life prediction tool. Hence strain energy release rate thresholds, G_{th}, below which no delamination would occur were also measured. Mode I and II threshold G values for no delamination growth were found by monitoring the number of cycles to delamination onset in the DCB and ENF specimens. The maximum applied G for which no delamination growth had occurred until at least 10^6 cycles was considered the threshold strain energy release rate. The G_{th} values for both mode I and mode II were much less than their corresponding fracture toughness. Results show that specimens that had been statically pre-cracked in shear have similar G_{th} values for mode I and mode II at R ratios of 0.1 and 0.5. An expression was developed which relates G_{th} and G_c to cyclic delamination growth rate. Comments are given on how testing effects, e.g. facial interference and damage ahead of the delamination front, may invalidate the experimental determination of the constants in the expression.

17. Key Words (Suggested by Author(s))
Composite materials
Delamination
Fatigue
Threshold
Strain energy release rate

18. Distribution Statement
Unclassified - Unlimited
Subject Category - 24

19. Security Classif. (of this report)	20. Security Classif. (of this page)	21. No. of Pages	22. Price*
Unclassified	Unclassified	51	A04

*For sale by the National Technical Information Service, Springfield, Virginia 22161